

14 **Abstract**

15 Conventionally, subsurface fluid flow modelling studies have concentrated on the
16 characterization of fracture networks and their capacity to facilitate vertical and lateral fluid
17 movements. This study utilizes unique field observations of oxidation halos in a well-bedded
18 carbonate sequence in the Paris Basin, France, offering new perspectives on fluid flow
19 pathways. It demonstrates that, in addition to fractures, bedding planes also serve as critical
20 conduits for horizontal fluid flow. This research highlights the importance of integrating both
21 fractures and bedding planes to assess connectivity and improve fluid flow models, particularly
22 in relatively shallow subsurface environments where such features are more likely to remain
23 open or become reactivated. This approach is vital for geoscience and engineering applications,
24 including reservoir management and waste disposal strategies.

25

26 **1 Introduction**

27 In tightly cemented sedimentary rocks, fractures are widely recognized as the primary
28 conduits for fluid flow, especially in environments where matrix permeability is low (Nelson,
29 1985). Consequently, common approaches to predicting subsurface fluid migration have
30 predominantly focused on characterizing fracture networks (Bourbiaux, 2010; De Dreuzy et al.,
31 2012; Lei et al., 2017). Conventionally, outcrop-scale data is utilized to inform larger-scale
32 subsurface flow models by assessing the geometric and topological properties of these fracture
33 networks (Odling et al., 1999; Agosta et al., 2010; Sanderson and Nixon, 2015; Wennberg et al.,
34 2016; Lei et al., 2017). These properties, typically measured directly at the outcrop scale, help
35 estimate the extent and scaling of these networks in the subsurface, thereby constraining flow
36 properties (Wilson et al., 2011; Zhu et al., 2021).

37 However, this well-established approach assumes that subsurface fluid flow is primarily
38 accommodated by fracture networks, which predominantly facilitate vertical and lateral fluid
39 movements. Consequently, it often neglects the potential for horizontal fluid movements that
40 could be facilitated, for example, by bedding planes—stratigraphic layers and/or interfaces
41 between layers. This neglect is largely due to the challenges associated with identifying these

42 horizontal fluid flow pathways, leading to an exclusive focus on fractures as the main conduits
43 for fluid flow.

44 The primary goal of this study is to highlight the often-overlooked importance of
45 bedding planes in fluid flow. Field observations from an exceptional exposure of oxidation halos
46 within a well-bedded carbonate sequence in the Paris Basin, France, provide critical insights
47 into past fluid flow pathways. Results suggest that bedding planes also play a crucial role as
48 pathways, and their interaction with sub-vertical fractures enhance the overall connectivity of
49 fluid systems. This finding highlights the necessity of integrating both fractures and bedding
50 planes into subsurface fluid flow models, especially in well-bedded sedimentary sequences.
51 Incorporation of bedding planes into flow models can therefore improve our understanding of
52 subsurface fluid dynamics, which is essential for various geoscientific and engineering
53 applications, including efficient reservoir management and waste disposal strategies (e.g., Bear
54 et al., 2012).

55 **2 Data and Methodology**

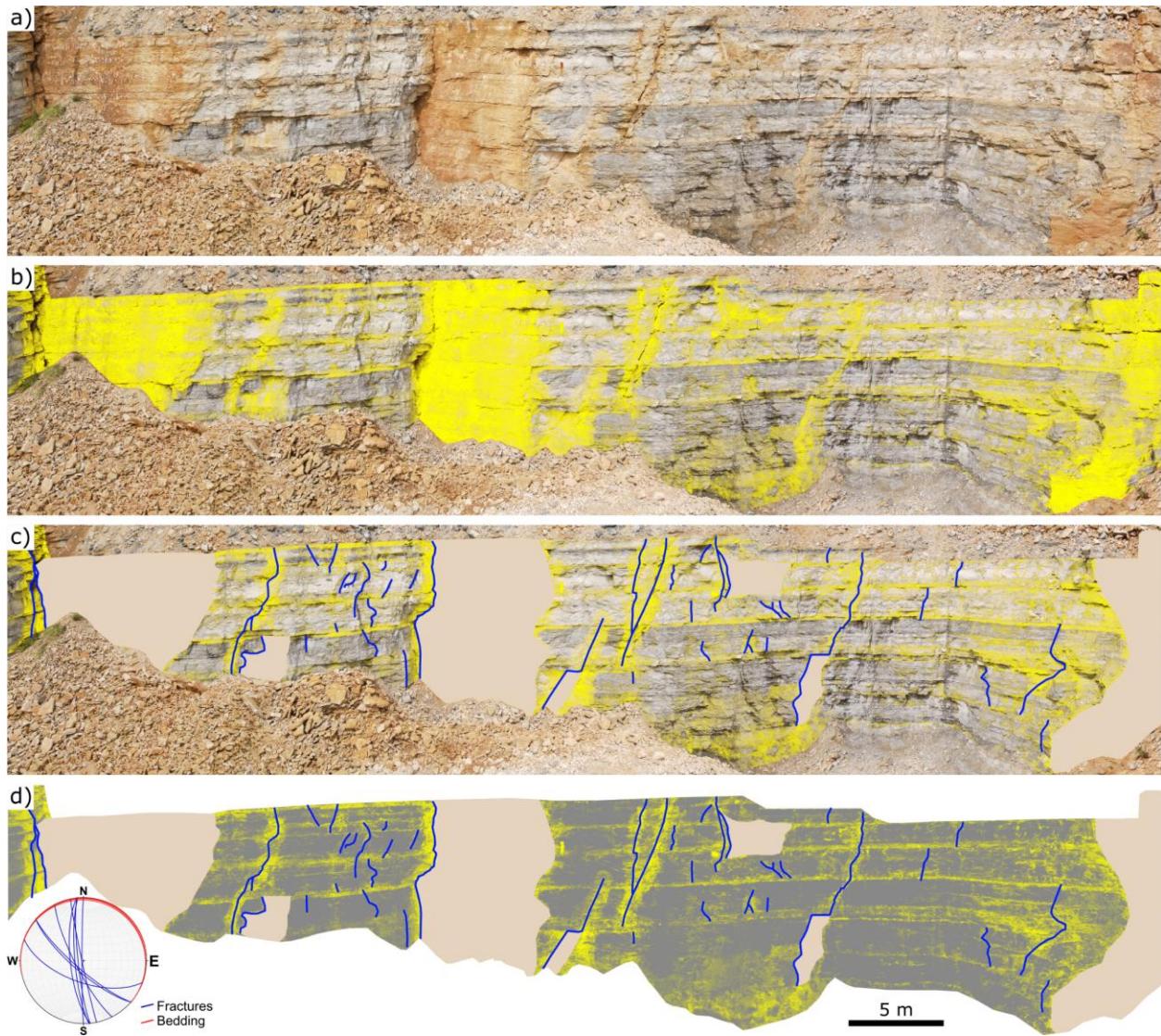
56 The study is based on an outcrop exposure within the Sommerécourt quarry at the
57 eastern Paris Basin, France. The Paris Basin is an intracratonic basin that experienced multiple
58 episodes of subsidence and sedimentation during the Mesozoic (Pomerol, 1978; Mégnien,
59 1980). This study focuses on the Dogger Formation, primarily composed of limestone and marl,
60 deposited during the Middle Jurassic and marking a transition from marine transgression to
61 more restricted lagoonal conditions (e.g., Brigaud et al., 2009). The formation is extensively
62 studied for its petroleum potential and geothermal resources in the Paris Basin (e.g., Lopez et
63 al., 2010) and its western continuation in the Upper Rhine Graben (e.g., Böcker et al., 2017).

64 On a more regional scale, the outcrop is located approximately 200 meters north of the
65 E-W striking Vittel fault, which forms part of the extensive Variscan Wight-Bray-Vittel
66 megastructure, extending over 700 km from the Bristol Channel to eastern France. This major
67 tectonic structure was reactivated during the Meso-Cenozoic period (Bergerat et al., 2007) and
68 has been reported as a major corridor for paleo-circulation of geothermal fluids within the Paris
69 Basin, facilitating connections between the Dogger and Triassic reservoirs (Bril et al., 1994).

70 In the studied outcrop, fractures exhibit approximately NW-SE strikes, with an average
71 dip of 80°, while the bedding planes are nearly horizontal, dipping on average 3° towards the
72 NNE (as shown in the inset in Figure 1). Oxidation halos, which serve as key indicators of past
73 fluid flow, are observed surrounding both fractures and bedding planes (Figure 1). A cut surface
74 of a rock sample and a thin section illustrating the oxidation halo in contrast to the non-
75 oxidized host rock are presented in Figure 2. This figure clearly shows the sharp transition from
76 the orange to reddish-brown hues of the oxidized zone to the greyish-blue and beige tones of
77 the non-oxidized host rock, further confirming the presence and intensity of oxidation halos at
78 a finer scale.

79 To enhance the examination of these halos, field observations were supplemented with
80 image processing techniques to improve their visibility. A virtual outcrop model (VOM) and a 2D
81 orthorectified image of the quarry working face were created from digital images collected by
82 an unmanned aerial vehicle (UAV). Subsequently, Inkscape software was used to apply a
83 fluorescence filter to increase the contrast between the halos and the surrounding rock matrix,
84 allowing for the detection of subtle oxidation variations that might otherwise go unnoticed.
85 Additionally, a saturation map filter was used to adjust colour intensities, further enhancing the
86 clarity of the halos. These image manipulations, combined with adjustments to contrast and
87 brightness, enabled more precise identification of the halos and allowed for detailed mapping
88 of both fractures and bedding planes that facilitated past fluid flow (Figures 1 and 3).

89 The resulting maps were used to analyse the connectivity and estimate the intensity and
90 density of fractures and bedding planes. Connectivity analysis involved mapping the spatial
91 distribution of three node types, as defined by Manzocchi (2002): isolated tips (I-nodes),
92 crossing fractures/bedding planes (X-nodes), and abutments or splays (Y-nodes). The
93 terminology by Dershowitz and Herda (1992) is followed for the intensity of fractures and/or
94 bedding planes (P21), which is defined as the length per unit area, and their density (P20),
95 which is defined as the number of features per unit area. These metrics were calculated using
96 the method of Mauldon et al. (2001) and implemented with FracPaq v. 2.8 (Healy et al., 2017).



97

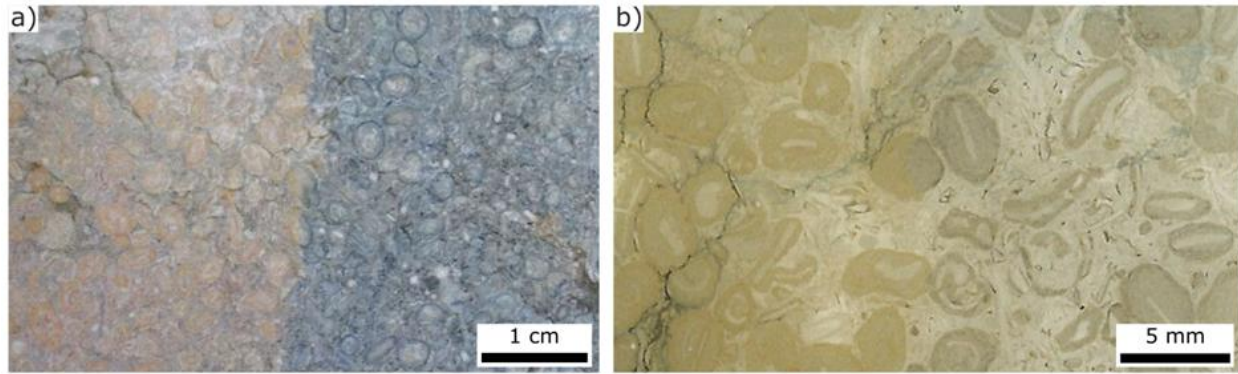
98 **Figure 1.** (a) Panoramic view of the studied outcrop. (b) Image processing enhances the visibility

99 of oxidation halos, highlighted in yellow. (c) Fracture traces are shown in blue, while fracture

100 surfaces are marked in brown. (d) Same as (c), but without the original image background. The

101 inset shows the orientation of fractures and bedding planes as great circles on a lower

102 hemisphere, equal-area projection.



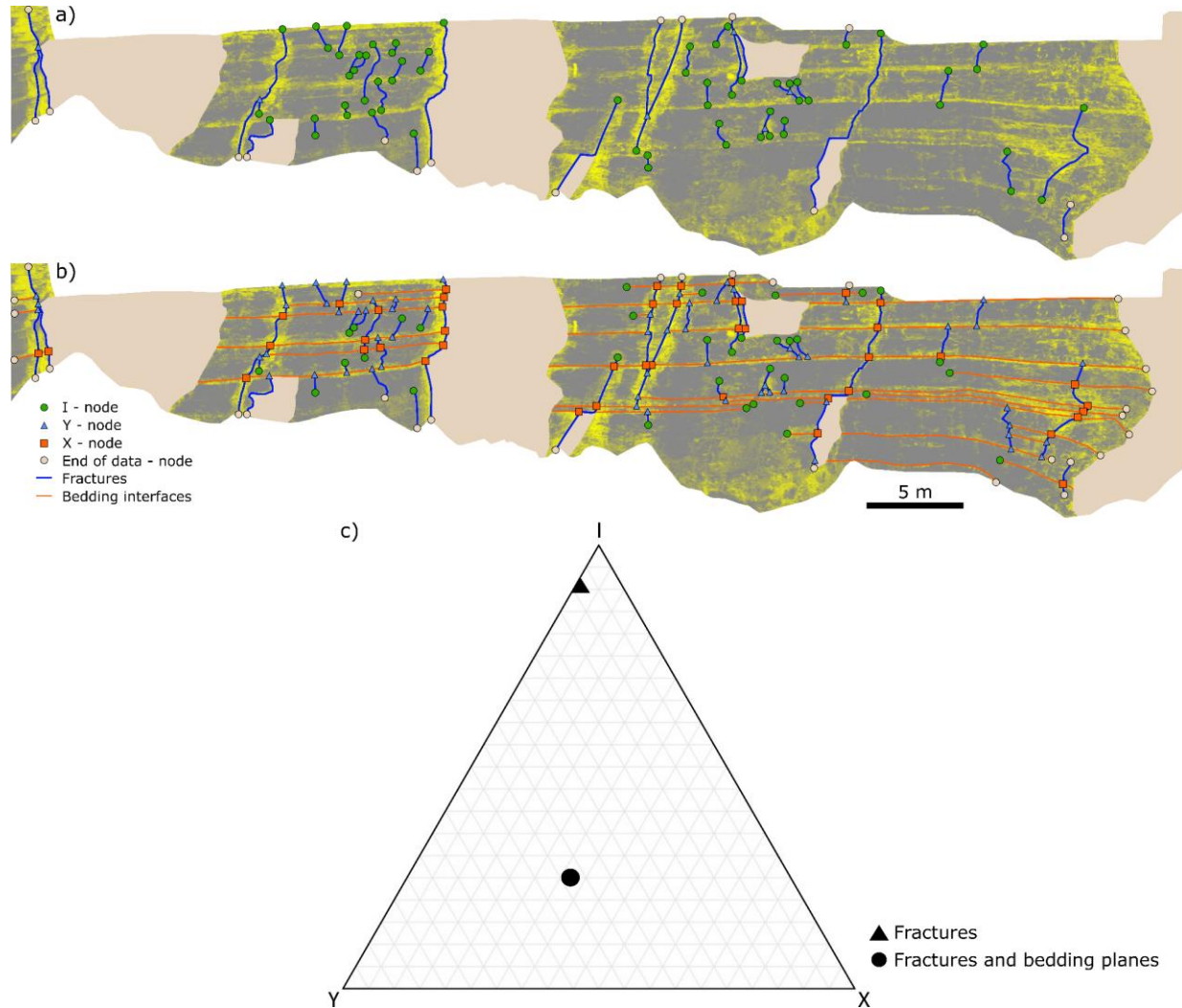
103

104 **Figure 2.** (a) Cut surface of the rock sample and (b) thin section showing both the oxidation halo
105 (left side) and the non-oxidized host rock (right side). A sharp transition from the orange to
106 reddish-brown hues of the oxidized zone to the grayish-blue and beige tones of the non-
107 oxidized host rock is observed.

108 **3 Results**

109 This section highlights the critical importance of integrating both fractures and bedding
110 planes when analyzing fluid flow in sedimentary formations, particularly in relatively shallow
111 carbonate sequences, as demonstrated by the present case study. Figure 3 (a and b) presents
112 connectivity maps comparing two different scenarios: (a) fractures only, and (b) both fractures
113 and bedding planes. These maps clearly demonstrate a marked increase in connectivity when
114 bedding planes are considered alongside fractures. Furthermore, Figure 3c shows a ternary plot
115 based on I-Y-X connectivity analysis (Manzocchi, 2002), comparing the fracture network alone
116 (from Figure 3a) with the combined network of fractures and bedding planes (from Figure 3b).
117 Networks showing improved connectivity are positioned towards the base of the triangle,
118 indicating a higher proportion of X and Y nodes. This shift towards the base in the combined
119 network plot highlights the enhanced connectivity provided by bedding planes, demonstrating
120 quantitatively how their inclusion can lead to more efficient fluid flow within the well-bedded
121 sedimentary sequence. This enhanced connectivity not only supplements the vertical pathways
122 provided by fractures but also introduces vital horizontal routes that could facilitate broader
123 fluid distribution across the formation. This effectively links isolated fractures, turning bedding
124 planes into critical conduits that increase overall system connectivity. It is worth noting,
125 however, that the aforementioned connectivity properties of the fracture network primarily

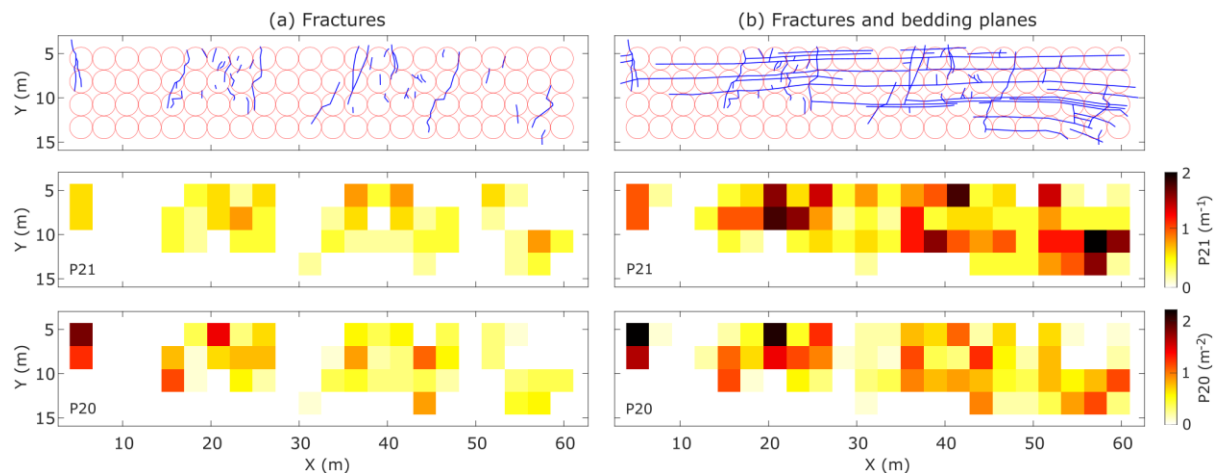
126 reflect only the vertical direction, influenced by the nature of the available data (e.g., cross-
127 sectional view of the quarry face). However, given the measured orientations of fractures (as
128 shown in the inset of Figure 1), the fracture network is expected to exhibit lateral connectivity,
129 which would further facilitate lateral fluid movements.



130

131 **Figure 3.** Connectivity maps showing the spatial distribution of different node types (I, Y and X)
132 for (a) fractures only, and (b) both fractures and bedding planes at the studied outcrop. (c)
133 Ternary plot of I-Y-X connectivity analysis (Manzocchi, 2002) comparing the fracture network
134 alone (as in a) with the combined fracture and bedding plane network (as in b) at the studied
135 outcrop. Better-connected networks are plotted toward the base of the triangle indicating a
136 higher proportion of X and Y nodes.

137 Maps of the estimated intensity and density of (a) fractures only and (b) both fractures
138 and bedding planes are presented in Figure 4. These maps indicate that areas with combined
139 fracture and bedding plane networks have higher P21 and P20 values, suggesting a denser and
140 potentially more permeable structure conducive to fluid migration. These parameters are
141 crucial as they directly influence the fluid flow properties of the formation, with higher values
142 generally indicative of increased potential for fluid storage and transport. Complementing the
143 connectivity maps shown in Figure 3, these P21 and P20 maps further demonstrate how
144 apparently isolated fracture corridors become interconnected through fluid flow along the
145 bedding planes.



146
147 **Figure 4.** Estimated fracture intensity (P21) and fracture density (P20) maps for (a) fractures
148 only, and (b) both fractures and bedding planes at the studied outcrop. Fracture traces and
149 fracture plus bedding plane traces (depicted in blue) are shown at the top, indicating the
150 locations of the scan circles used to estimate intensity (m^{-1}) and density (m^{-2}).

151 While this study demonstrates that bedding planes can serve as horizontal pathways for
152 fluid flow, they also have the capacity to restrict both fracture propagation and associated
153 vertical fluid movements. In Figure 5, the fracture on the right and its associated oxidation halo
154 terminate abruptly at a bedding plane, acting as a barrier to fluid migration below this plane
155 and to downward fracture propagation. Despite this abrupt termination, the presence of the
156 halo along the corresponding bedding plane indicates fluid flow along it, resulting in a Y-node
157 connection as shown in Figure 3. Conversely, the fracture on the left is not restricted by any

158 bedding plane, and its associated halo gradually terminates upwards, becoming well-rounded
159 at the fracture tip. These observations, further highlight the well-documented influence of
160 mechanical stratigraphy on fracture propagation across different bedding planes (e.g., Renshaw
161 and Pollard, 1995; McGinnis et al., 2017), illustrating the complex interplay between bedding
162 planes, fracture growth, and fluid dynamics.



163
164 **Figure 5.** Close-up photograph of the outcrop on the left, and the same image after processing
165 to enhance the visibility of oxidation halos, which are highlighted in yellow on the right.

166 **4 Discussion**

167 4.1 Factors controlling fluid flow along bedding planes

168 Through semi-quantitative analysis involving geometrical and topological assessments,
169 this study demonstrates that bedding planes not only complement the vertical and lateral fluid
170 pathways provided by fractures but also significantly enhance system connectivity through
171 horizontal routes.

172 The factors controlling fluid flow along bedding planes in the studied area have not yet
173 been fully identified. However, preliminary observations suggest that dissolution processes,
174 particularly pressure-solution of the cement between detrital and precipitated grains, are likely
175 responsible for the development of porosity and permeability within the marly limestone
176 layers.

177 Previous research on fluid flow along bedding planes, although less common than
178 studies on fractures, primarily focuses on phenomena such as karstification and cave genesis
179 (Cooke et al., 2006; Filipponi et al., 2010; Sauro et al., 2013; Frumkin et al., 2017; Roded et al.,
180 2024). For example, Filipponi et al. (2010) identified three distinct types of inception horizons
181 that promote cave development and, consequently, concentrate fluid flow. These types are
182 differentiated by differences in permeability and the presence of fractures along bedding
183 interfaces. Additionally, Sauro et al. (2013) reported that flexural slip surfaces between beds
184 are particularly conducive to the development of conduits and deep karst systems. In another
185 study focusing on hydrocarbon migration, Noufal and Obaid (2017) noted that sheared bedding
186 planes acted as primary corridors in the migration of hydrocarbons within Abu Dhabi's
187 sedimentary basins. Furthermore, Skurtveit et al. (2021) found that the fractures along bedding
188 interfaces and the petrophysical properties of the rock sequence-controlled layer-parallel CO₂
189 migration away from fault zones, which serve as the main pathways for CO₂ migration in
190 Humbug Flats, Utah, USA. A recurrent theme in all these studies is the role of shearing and
191 fracturing along bedding interfaces in promoting bed-parallel fluid flow. Given that bed-parallel
192 shearing is quite commonly observed in both compressional (e.g., Sanderson, 1982; Tanner,
193 1989) and extensional (e.g., Delogkos et al., 2022) tectonic settings, it is plausible that such
194 shearing can also enhance fluid flow along these bedding planes, particularly in relatively
195 shallow subsurface environments where such features are more likely to remain open or
196 become reactivated.

197 While bedding planes acting as secondary permeability features can promote bed-
198 parallel fluid flow, other mechanisms, including contrasts in petrophysical properties (e.g.,
199 Filipponi et al., 2010) and sedimentological processes, may also facilitate such flow. For
200 example, Cooke et al. (2006) concluded that continuous flow along bedding planes may

201 promote dissolution, which over time could lead to development of regionally extensive, bed-
202 parallel, high-permeability features. Frumkin et al. (2017) also observed that bedding planes
203 can initially have sub-millimetre to sub-centimetre width, which subsequently increases due to
204 dissolution enlargement. Furthermore, Golab et al. (2017) reported that bioturbation-
205 influenced porosity enhances horizontal fluid flow within a carbonate platform system in
206 otherwise low porosity and permeability sediments. Finally, it is worth mentioning that
207 horizontal fluid flow pathways can be highly variable in three dimensions due to the inherent
208 variability of petrophysical and sedimentological properties. Thomas et al. (2021) demonstrated
209 the presence of such three-dimensional heterogeneities of facies, porosity, and permeability
210 within the Middle Jurassic carbonate reservoirs in Paris Basin.

211 Additionally, the presence of karstification features in the examined area is noteworthy,
212 as it can significantly influence subsurface fluid flow by potentially complicating pre-existing
213 pathways and enhancing permeability and connectivity (e.g., Moore and Walsh, 2021). This
214 highlights the complex, multifaceted nature of fluid flow in the subsurface and emphasizes the
215 necessity of integrating various geological features and processes in subsurface flow modelling -
216 an aspect often underestimated in prior studies.

217 4.2 Conditions of formation of oxidation halos

218 Oxidation halos are typically associated with shallow subsurface conditions, where
219 oxidizing fluids circulate, but their depth range can vary depending on the fluid source and
220 redox conditions. In most cases, oxidation halos form due to meteoric groundwater infiltration,
221 generally within the upper few hundred meters of the subsurface (0–500 m). However,
222 oxidation at greater depths can also occur when oxidized fluids originate from deep-seated
223 reservoirs, such as hydrothermal systems or basinal brines (e.g., Grare et al., 2018).

224 In the studied area, XRF measurements of rock samples indicate that iron content
225 remains similar in both the oxidized zone and the host rock, with values ranging between 7000
226 and 8000 ppm. This suggests that iron was not significantly leached or transported, but rather
227 that oxygen introduced through meteoric groundwater infiltration converted Fe^{2+} to Fe^{3+} in situ
228 at relatively shallow depths.

229 Although oxidation halos can, in certain settings, form under stagnant water conditions
230 (Balsamo et al., 2013), observations in the studied area suggest a different scenario. The
231 oxidation halos exhibit elongated and interconnected patterns that align with structural
232 discontinuities, such as bedding planes and fractures. This geometry, which reflects structural
233 anisotropy, is more characteristic of advective flow pathways, where fluids migrate through
234 preferential conduits rather than diffusing isotropically in stagnant conditions.

235 Furthermore, if oxidation had occurred under fully stagnant conditions, Fe oxidation
236 would be expected to be uniform throughout the rock mass. However, XRF measurements
237 indicate that iron content remains similar across the entire rock mass, confirming that iron was
238 not leached or transported in significant amounts. The fact that oxidation is localized along
239 fractures and bedding planes suggests that an oxidizing (O-rich) fluid must have circulated
240 advectively, even if the surrounding rock was immersed in a stagnant, reduced water
241 environment.

242 Future geochemical and isotopic analyses could further refine this interpretation and
243 provide a more detailed understanding of the fluid origins and migration history.

244 4.3 Implications

245 Although, the examined oxidation halos are potentially associated with near-surface
246 conditions, the fundamental processes governing fluid flow, connectivity, and permeability are
247 not necessarily depth-dependent. The oxidation halos in our study serve as natural tracers of
248 paleo-fluid pathways, providing direct evidence of preferential flow along bedding planes. This
249 has implications for deeper subsurface reservoirs, where similar structural and stratigraphic
250 controls on fluid migration can be expected. Therefore, despite the shallow setting of our
251 dataset, the observed fluid flow patterns provide insights into permeability anisotropy, which
252 can be extrapolated to deeper subsurface environments, where direct observations are
253 inherently limited.

254 The findings of this study, therefore, can have significant implications for various
255 subsurface activities. Reservoir models that focus exclusively on fractures may underestimate
256 fluid storage and transport potential, potentially leading to suboptimal decisions in reservoir

257 management or waste disposal. By incorporating bedding planes into fluid flow models,
258 predictions of fluid movement in reservoirs and aquifers can become more accurate, which is
259 crucial for effective (a) resource extraction, including groundwater, geothermal energy, and
260 hydrocarbons, and (b) environmental management, such as carbon capture and storage (CCS)
261 and contamination control. For example, in geothermal energy production, understanding the
262 dual role of fractures and bedding planes can refine recovery strategies by optimizing well
263 placements and enhancing recovery methods. This is particularly valuable for the Paris Basin,
264 known for its geothermal energy resources, as well as for other basins where the Dogger
265 Formation is present and exhibits high geoenergy potential, such as the Upper Rhine Graben.
266 Furthermore, the findings of this study can contribute to a deeper understanding of
267 fundamental geological processes such as karstification, speleogenesis, and diagenesis,
268 advancing our knowledge of their development and distribution.

269 **5 Conclusions**

270 The examination of the exceptionally well exposed oxidation halos within the well-
271 bedded carbonate sequence in the Paris Basin, France, reveals that subsurface fluid flow is
272 more complex than previously understood. This study demonstrates that fluids can
273 preferentially flow horizontally along bedding planes, complementing vertical and lateral flows
274 along fracture networks. Bedding planes thus can act as critical conduits for fluid migration,
275 especially in regions with low fracture density or poorly connected fractures. This challenges
276 the conventional focus solely on fractures and highlights the need for bedding planes to be
277 more thoroughly considered in fluid flow models.

278

279 **Acknowledgments**

280 This work was supported by a French government grant managed by the Agence Nationale de
281 la Recherche under the France 2030 initiative, reference ANR-22-EXSS-0010. The authors would
282 like to extend their gratitude to Guy Calin for granting permission to conduct research in the
283 quarry, and to the quarry employees for their hospitality. We also thank Cedric Bailly, Jocelyn
284 Barbarand, Thomas Blaise, Benjamin Brigaud, Yves Missenard, and Bertrand Saint-Bezar,

This manuscript has been accepted for publication in Journal of the Geological Society ([link](#)). Please note that, despite having undergone peer-review, the final manuscript has yet to be edited and typeset and may be different to the published version.

285 members of the Relief, Bassins et Ressources (RBR) group at GEOPS, Université Paris-Saclay, for
286 their insightful discussions on this topic. Additionally, we acknowledge Giovanni Camanni for
287 reviewing an earlier version of this manuscript and Philippe Boulvais for providing insights into
288 fluid-rock interactions. We thank one anonymous reviewer and Stefano Tavani for their useful
289 comments and Alexandra Tamas for editorial handling.

290

291 **Open Research - Availability Statement**

292 A textured 3D virtual outcrop model (VOM) of the studied outcrop is available for exploration
293 and download on the Sketchfab repository at: <https://skfb.ly/pqSwC>.

294

295 **References**

- 296 Agosta, F., Alessandroni, M., Antonellini, M., Tondi, E. and Giorgioni, M., 2010. From fractures
297 to flow: A field-based quantitative analysis of an outcropping carbonate reservoir.
298 *Tectonophysics*, 490(3-4), pp.197-213.
- 299 Balsamo, F., Bezerra, F.H.R., Vieira, M.M. and Storti, F., 2013. Structural control on the
300 formation of iron-oxide concretions and Liesegang bands in faulted, poorly lithified Cenozoic
301 sandstones of the Paraíba Basin, Brazil. *Bulletin*, 125(5-6), pp.913-931.
- 302 Bear, J., Tsang, C.F. and De Marsily, G., 2012. *Flow and contaminant transport in fractured rock*.
303 Academic Press.
- 304 Bergerat, F., Elion, P., De Lamotte, D.F., Proudhon, B., Combes, P., André, G., Willeveau, Y.,
305 Laurent-Charvet, S., Kourdian, R., Lerouge, G. and d'Estevou, P.O., 2007. 3D multiscale
306 structural analysis of the eastern Paris basin: the Andra contribution. *Mém. Soc. Géol. France*,
307 178, pp.15-35.
- 308 Böcker, J., Littke, R. and Forster, A., 2017. An overview on source rocks and the petroleum
309 system of the central Upper Rhine Graben. *International Journal of Earth Sciences*, 106, pp.707-
310 742.
- 311 Bourbiaux, B., 2010. Fractured reservoir simulation: a challenging and rewarding issue. *Oil &*
312 *Gas Science and Technology—Revue de l'Institut Français du Pétrole*, 65(2), pp.227-238.

- 313 Brigaud, B., Durllet, C., Deconinck, J. F., Vincent, B., Puc at, E., Thierry, J., & Trouiller, A. (2009).
314 Facies and climate/environmental changes recorded on a carbonate ramp: a sedimentological
315 and geochemical approach on Middle Jurassic carbonates (Paris Basin, France). *Sedimentary*
316 *Geology*, 222(3-4), 181-206.
- 317 Bril, H., Velde, B., Meunier, A. and Iqdari, A., 1994. Effects of the “pays de bray” fault on fluid
318 paleocirculations in the Paris basin dogger reservoir, France. *Geothermics*, 23(3), pp.305-315.
- 319 Cooke, M.L., Simo, J.A., Underwood, C.A. and Rijken, P., 2006. Mechanical stratigraphic controls
320 on fracture patterns within carbonates and implications for groundwater flow. *Sedimentary*
321 *Geology*, 184(3-4), pp.225-239.
- 322 De Dreuzy, J.R., M eheust, Y. and Pichot, G., 2012. Influence of fracture scale heterogeneity on
323 the flow properties of three-dimensional discrete fracture networks (DFN). *Journal of*
324 *Geophysical Research: Solid Earth*, 117(B11).
- 325 Delogkos, E., Roche, V. and Walsh, J.J., 2022. Bed-parallel slip associated with normal fault
326 systems. *Earth-Science Reviews*, 230, p.104044.
- 327 Dershowitz, W.S. and Herda, H.H., 1992, June. Interpretation of fracture spacing and intensity.
328 In ARMA US rock mechanics/geomechanics symposium (pp. ARMA-92). ARMA.
- 329 Filipponi, M., Jeannin, P.Y. and Tacher, L., 2010. Understanding cave genesis along favourable
330 bedding planes. The role of the primary rock permeability. *Zeitschrift f ur Geomorphologie.*
331 *Supplementband*, 54(2), p.91.
- 332 Frumkin, A., Langford, B., Lisker, S. and Amrani, A., 2017. Hypogenic karst at the Arabian
333 platform margins: Implications for far-field groundwater systems. *Bulletin*, 129(11-12), pp.1636-
334 1659.
- 335 Golab, J.A., Smith, J.J., Clark, A.K. and Morris, R.R., 2017. Bioturbation-influenced fluid pathways
336 within a carbonate platform system: the Lower Cretaceous (Aptian–Albian) Glen Rose
337 Limestone. *Palaeogeography, Palaeoclimatology, Palaeoecology*, 465, pp.138-155.
- 338 Grare, A., Lacombe, O., Mercadier, J., Benedicto, A., Guilcher, M., Trave, A., Ledru, P. and
339 Robbins, J., 2018. Fault zone evolution and development of a structural and hydrological
340 barrier: the quartz breccia in the Kiggavik Area (Nunavut, Canada) and its control on uranium
341 mineralization. *Minerals*, 8(8), p.319.

- 342 Healy, D., Rizzo, R.E., Cornwell, D.G., Farrell, N.J., Watkins, H., Timms, N.E., Gomez-Rivas, E. and
343 Smith, M., 2017. FracPaQ: A MATLAB™ toolbox for the quantification of fracture patterns.
344 Journal of Structural Geology, 95, pp.1-16.
- 345 Lei, Q., Latham, J.P. and Tsang, C.F., 2017. The use of discrete fracture networks for modelling
346 coupled geomechanical and hydrological behaviour of fractured rocks. Computers and
347 Geotechnics, 85, pp.151-176.
- 348 Lopez, S., Hamm, V., Le Brun, M., Schaper, L., Boissier, F., Cotiche, C. and Giuglaris, E., 2010. 40
349 years of Dogger aquifer management in Ile-de-France, Paris Basin, France. Geothermics, 39(4),
350 pp.339-356.
- 351 Manzocchi, T., 2002. The connectivity of two-dimensional networks of spatially correlated
352 fractures. Water Resources Research, 38(9), pp.1-1.
- 353 Mauldon, M., Dunne, W.M. and Rohrbaugh Jr, M.B., 2001. Circular scanlines and circular
354 windows: new tools for characterizing the geometry of fracture traces. Journal of structural
355 geology, 23(2-3), pp.247-258.
- 356 McGinnis, R.N., Ferrill, D.A., Morris, A.P., Smart, K.J. and Lehrmann, D., 2017. Mechanical
357 stratigraphic controls on natural fracture spacing and penetration. Journal of Structural
358 Geology, 95, pp.160-170.
- 359 Mégnién, C., 1980. Synthèse géologique du Bassin de Paris, I, Stratigraphie et paléogéographie.
360 In: Mémoires du Bureau de Recherches Géologiques et Minières, vol. 101, 466 pp.
- 361 Moore, J.P. and Walsh, J.J., 2021. Quantitative analysis of Cenozoic faults and fractures and
362 their impact on groundwater flow in the bedrock aquifers of Ireland. Hydrogeology Journal,
363 29(8), pp.2613-2632.
- 364 Nelson, R.A., 1985. Geologic analysis of naturally fractured reservoirs (Vol. 1). Gulf Professional
365 Publishing.
- 366 Noufal, A. and Obaid, K., 2017, November. Bedding Corridors as Migration Pathways in Abu
367 Dhabi Fields. In Abu Dhabi International Petroleum Exhibition and Conference (p.
368 D011S003R003). SPE.
- 369 Odling, N.E., Gillespie, P., Bourguine, B., Castaing, C., Chiles, J.P., Christensen, N.P., Fillion, E.,
370 Genter, A., Olsen, C., Thrane, L. and Trice, R., 1999. Variations in fracture system geometry and

371 their implications for fluid flow in fractures hydrocarbon reservoirs. *Petroleum Geoscience*,
372 5(4), pp.373-384.

373 Pomerol, C., 1978. Paleogeographic and structural evolution of the Paris Basin, from the
374 Precambrian to the present day, in relation to neighboring regions. *Geologie En Mijnbouw*
375 *Journal of Geosciences*, 57, pp.533-543.

376 Renshaw, C.E. and Pollard, D.D., 1995, April. An experimentally verified criterion for
377 propagation across unbounded frictional interfaces in brittle, linear elastic materials. In
378 *International journal of rock mechanics and mining sciences & geomechanics abstracts* (Vol. 32,
379 No. 3, pp. 237-249). Pergamon.

380 Roded, R., Langford, B., Aharonov, E., Szymczak, P., Ullman, M., Yaaran, S., Lazar, B., Frumkin,
381 A., 2024. Hypogene speleogenesis in carbonates by cooling, confined hydrothermal flow: The
382 case of Mt. Berenike caves, Israel. *International Journal of Speleology*, 53(2), 191-209.

383 Sanderson, D.J., 1982. Models of strain variation in nappes and thrust sheets: a review.
384 *Tectonophysics*, 88(3-4), pp.201-233.

385 Sanderson, D.J. and Nixon, C.W., 2015. The use of topology in fracture network
386 characterization. *Journal of Structural Geology*, 72, pp.55-66.

387 Sauro, F., Zampieri, D. and Filipponi, M., 2013. Development of a deep karst system within a
388 transpressional structure of the Dolomites in north-east Italy. *Geomorphology*, 184, pp.51-63.

389 Skurtveit, E., Torabi, A., Sundal, A. and Braathen, A., 2021. The role of mechanical stratigraphy
390 on CO₂ migration along faults—examples from Entrada Sandstone, Humberg Flats, Utah, USA.
391 *International Journal of Greenhouse Gas Control*, 109, p.103376.

392 Tanner, P.G., 1989. The flexural-slip mechanism. *Journal of Structural Geology*, 11(6), pp.635-
393 655.

394 Thomas, H., Brigaud, B., Blaise, T., Saint-Bezar, B., Zordan, E., Zeyen, H., Andrieu, S., Wennberg,
395 O.P., Casini, G., Jonoud, S. and Peacock, D.C., 2016. The characteristics of open fractures in
396 carbonate reservoirs and their impact on fluid flow: a discussion. *Petroleum Geoscience*, 22(1),
397 pp.91-104.

This manuscript has been accepted for publication in Journal of the Geological Society ([link](#)).
Please note that, despite having undergone peer-review, the final manuscript has yet to be edited and typeset and may be different to the published version.

398 Vincent, B., Chirol, H., Portier, E. and Mouche, E., 2021. Contribution of drone photogrammetry
399 to 3D outcrop modeling of facies, porosity, and permeability heterogeneities in carbonate
400 reservoirs (Paris Basin, Middle Jurassic). *Marine and Petroleum Geology*, 123, p.104772
401 Wilson, C.E., Aydin, A., Karimi-Fard, M., Durlofsky, L.J., Amir, S., Brodsky, E.E., Kreylos, O. and
402 Kellogg, L.H., 2011. From outcrop to flow simulation: Constructing discrete fracture models
403 from a LIDAR survey. *AAPG bulletin*, 95(11), pp.1883-1905.
404 Zhu, W., Khirevich, S. and Patzek, T.W., 2021. Impact of fracture geometry and topology on the
405 connectivity and flow properties of stochastic fracture networks. *Water Resources Research*,
406 57(7), p.e2020WR028652.